CLINICAL GENETICS An International Journal of Genetics, Molecular and Personalized Medicine

Clin Genet 2012: 81: 399–402
Printed in Singapore. All rights reserved

CLINICAL GENETICS
doi: 10.1111/j.1399-0004.2011.01733.x

Letter to the Editor

Association of genomic deletions in the *STXBP1* gene with Ohtahara syndrome

To the Editor:

Ohtahara syndrome (OS) is characterized by early-onset of seizures, suppression-burst patterns on electroencephalogram (EEG), and severe psychomotor retardation (1–3). *De novo* mutations in the *STXBP1* gene, including various point mutations and one complete deletion, have been found in about one-third of Japanese cases of cryptogenic OS (4–6). However, the clinical spectrum of *STXBP1* mutations can be applied to other pathologies. For instance, in one study, *STXBP1* abnormalities including a microdeletion were detected in approximately 10% of patients (5/49) with early-onset epileptic encephalopathy that did not fit into a specific epilepsy syndrome (7). Other studies have also detected *de novo STXBP1* mutations in 2 of 95 individuals with mental retardation and non-syndromic epilepsy (8), in addition to the detection of a *de novo* partial deletion in a child with epilepsy and autistic features (9, 10). On the basis of these findings, extensive genetic testing including copy number analysis of *STXBP1* should be considered in children with early-onset seizures. However, the use of high-resolution copy number analysis of *STXBP1* thus far has been limited.

In this study, we performed customized array comparative genomic hybridization (aCGH) analysis, in which a total of 27,026 probes covering the *STXBP1* locus (UCSC coordinates, May 2006: Chr9: 129,350,808–129,558,072 bp) were distributed with 5-bp spacing except for repeating element regions (Roche NimbleGen, Tokyo, Japan). Among the 28 patients with cryptogenic OS tested, we found pathogenic *de novo* deletions in two patients (7.1%), where one 4.6-kb deletion included only exon 4, and the other 2.85-Mb one involved the entire *STXBP1* gene (Table 1).

Patient 1506, a product of unrelated healthy parents, had no problems in the perinatal period. Tonic seizures with a flexion of the upper extremities started at 32 days of age, and frequent myoclonic seizures subsequently appeared. On the basis of suppression-burst pattern on EEG, the patient was diagnosed as having OS or early myoclonic encephalopathy (EME), which is another epileptic syndrome showing suppression-burst pattern on EEG (11). As OS and EME have common features, they can be difficult to distinguish (2, 3). Brain magnetic resonance imaging (MRI) revealed normal neuroanatomy. High-dose phenobarbital was able to effectively reduce the frequency of seizures. Customized aCGH and breakpoint polymerase chain reaction (PCR) analyses detected a *de novo* 4635-bp deletion involving exon 4 of the *STXBP1* gene (Fig. 1a–c). The presence of a 2-bp microhomology at the deletion junction suggested non-homologous recombination leading to a

Table 1. Copy number alterations found in OS patients

	Findings of customized aCGH and 2.7M array (upper)/sequence-confirmed rearrangements (lower)						
Patient	Aberrations	Start (bp)	End (bp)	Size (bp)	Genes	Inheritance	Origin
1506	Deletion	129,457,591	129,462,084	4493	*STXBP1*(Ex4)	*De novo*	Unknown[a]
		129,457,463	129,462,098	4635	—	—	—
2231	Deletion	129,020,847	131,869,806	2,848,959	70 RefSeq genes including *STXBP* and *SPTAN1*	*De novo*	Paternal[b]
		129,020,309	131,870,400	2,850,091		—	—

aCGH, array comparative genomic hybridization; OS, Ohtahara syndrome.
[a]No informative markers were available within the 4.6-kb region corresponding to the deletion.
[b]Examined by the *D9S918* (UCSC coordinates, May 2006: Chr9: 129,497,050–129,497,376 bp) microsatellite marker.

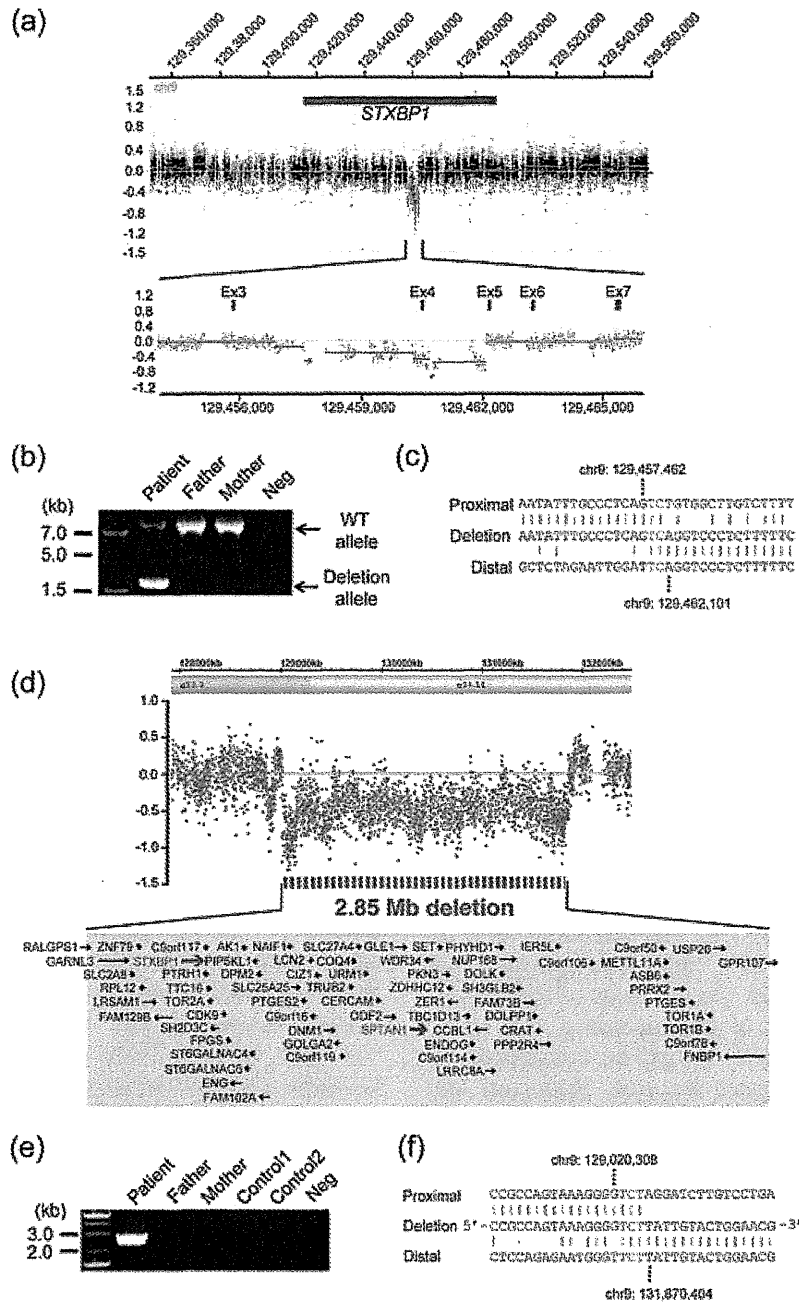

Fig. 1. The detection of two microdeletions using microarray. (**a**) A customized array comparative genomic hybridization (aCGH) profile of *STXBP1* locus in patient 1506. *x*- and *y*-axis show the genomic location from the p telomere of chromosome 9 (UCSC coordinates, May, 2006) and $\log_2$ (Cy3/Cy5 signal ratio) values (green dots ≥ 0.25; $-0.25 <$ black dots < 0.25; red dots ≤ -0.25), respectively (top panel). A close up view of the aCGH profile along with maps of the *STXBP1* exons (blue rectangles), showing the deletion of exon 4 (bottom panel). (**b**) Polymerase chain reaction (PCR) analysis of the family of patient 1506. Primers flanking the deletion amplified both 6398- and 1763-bp products from the wild type and deletion alleles, respectively, of the patient. However, the patient's parents had only a 6398-bp product, indicating the presence of a *de novo* deletion (Neg, negative control which contained no template DNA). (**c**) The deletion junction sequence. The top, middle and bottom strands show the proximal, deleted, and distal sequences, respectively. The two overlapping nucleotides are colored in red. (**d**) The 2.7M array profile clearly showed a 2.85-Mb deletion at 9q33.3-34.11 found in patient 2231 (top panel). A total of 70 RefSeq genes, including *STXBP1* and *SPTAN1*, were mapped within the deletion (bottom panel). (**e**) The breakpoint PCR analysis of the family of patient 2231. Primers flanking the deletion successfully amplified a 2430-bp product from the patient, indicating that the deletion occurred *de novo* (Neg, negative control that contained no template DNA). (**f**) The deletion junction sequence. The top, middle and bottom strands show the proximal, deleted and distal sequences, respectively. The three overlapping nucleotides are colored in red. The PCR conditions and primer sequences are available on request.

rearrangement (Fig. 1c) (12). The deletion of exon 4 was also confirmed by reverse transcriptase-PCR (Fig. S1, Supporting Information).

Patient 2231 was born at term after *in vitro* fertilization and embryo transfer. The body weight at birth was 2134 g (−2.4 SD), height 44.5 cm (−2.3 SD), and head circumference 32.0 cm (−0.8 SD). Multiple anomalies including cleft lip and palate, ventricular septal defect, overlapping fingers, and small penis were noted. G-banded chromosomal analysis was normal. The patient had an onset of sudden crying at 1 week of age followed by a cluster of epileptic spasms with suppression-burst pattern on EEG at 1 month. A brain MRI at 2 months showed a thin corpus callosum and relatively small cerebellum. After treatment with antiepileptic drugs proved ineffective, a ketogenic diet reduced the frequency of seizures. At 19 months, he showed spastic quadriplegia and profound intellectual disability at the level of a 2-month old. Customized aCGH, subsequent whole-genome 2.7M Array (Affymetrix, Santa Clara, CA), and breakpoint PCR analyses found a *de novo* 2.85-Mb microdeletion including *STXBP1* and *SPTAN1* (13) (Fig. 1d–f). The presence of a 3-bp homology at the deletion junction further suggested non-homologous recombination leading to the rearrangement (Fig. 1f).

In conclusion, our high-resolution copy number analysis in *STXBP1* locus revealed a 4.6-kb deletion encompassing only exon 4, which strongly suggests that copy number analysis covering all *STXBP1* exons should be recommended as a genetic test for children with early-onset seizures.

Supporting Information

The following Supporting information is available for this article:

Fig. S1. Examination of the mutated transcripts in lymphoblastoid cell lines derived from the patient 1506. (**a**) Reverse transcriptase polymerase chain reaction (RT-PCR) analysis of the patient with an exon 4 deletion relative to a normal control. A schematic representation of the transcript from exons 3 to 6 of *STXBP1* is indicated (top). The exons and primers are depicted as boxes and arrows, respectively. Two PCR products were amplified from the patient's cDNA: the upper was a wild-type (WT) transcript and the lower was the deleted mutant (middle). Only a single WT amplicon was detected in the control. The mutant amplicon was significantly increased by 30 μM cycloheximide (CHX) treatment for 4 h compared to dimethyl sulfoxide treatment as a vehicle control. RT (+): with reverse transcriptase, RT (−): without reverse transcriptase as a negative control. The sequence of the smaller amplicon clearly demonstrated exon 4 deletion (bottom). (**b**) Quantitative analysis of the nonsense-mediated mRNA decay (NMD) inhibition by CHX based on the data shown in (**a**). *p = 0.0023 by unpaired two tailed Student's *t*-test. Averages of duplicated experiments using two distinctive RNA samples are shown with error bars (SD). The mutant transcript lacking exon 4 created a premature stop codon at position 64, and suffered from degradation by NMD in the patient's lymphoblastoid cells. PCR conditions and the primer sequences are available on request.

Additional Supporting information may be found in the online version of this article.

Please note: Wiley-Blackwell Publishing is not responsible for the content or functionality of any supplementary materials supplied by the authors. Any queries (other than missing material) should be directed to the corresponding author for the article.

Acknowledgements

We would like to thank the patients and their families for their participation in this study. This work was supported by Research Grants from the Ministry of Health, Labour and Welfare (H. S., M. K., N. M. and N. M.), a Grant-in-Aid for Scientific Research from the Japan Society for the Promotion of Science (M. K. and N. M.), a Grant-in-Aid for Young Scientist from Japan Society for the Promotion of Science (H. S.), Research Promotion Fund from Yokohama Foundation for Advancement of Medical Science (H. S.), Research Grants from the Japan Epilepsy Research Foundation (H. S. and M. K.), and a Research Grant from Naito Foundation (N. M.).

H Saitsu[a]* *M Kato*[b]* *M Shimono*[c] *A Senju*[d] *S Tanabe*[d] *T Kimura*[d] *K Nishiyama*[a] *Y Yoneda*[a] *Y Kondo*[a] *Y Tsurusaki*[a] *H Doi*[a] *N Miyake*[a] *K Hayasaka*[b] *N Matsumoto*[a]

[a]Department of Human Genetics, Yokohama City University Graduate School of Medicine, Yokohama, Japan,

[b]Department of Pediatrics, Yamagata University Faculty of Medicine, Yamagata, Japan,

[c]Department of Pediatrics, School of Medicine, University of Occupational and Environmental Health, Kitakyushu, Japan, and

[d]Department of Pediatrics, Nihonkai General Hospital, Sakata, Japan

*These two authors contributed equally to this work.

References

1. Ohtahara S, Ishida T, Oka E et al. On the specific age dependent epileptic syndrome: the early-infantile epileptic encephalopathy with suppression-burst. No to Hattatsu 1976: 8: 270–279.
2. Djukic A, Lado FA, Shinnar S, Moshe SL. Are early myoclonic encephalopathy (EME) and the Ohtahara syndrome (EIEE) independent of each other? Epilepsy Res 2006: 70 (Suppl. 1): S68–S76.
3. Ohtahara S, Yamatogi Y. Ohtahara syndrome: with special reference to its developmental aspects for differentiating from early myoclonic encephalopathy. Epilepsy Res 2006: 70 (Suppl. 1): S58–S67.
4. Saitsu H, Kato M, Mizuguchi T et al. *De novo* mutations in the gene encoding STXBP1 (MUNC18-1) cause early infantile epileptic encephalopathy. Nat Genet 2008: 40: 782–788.
5. Saitsu H, Kato M, Okada I et al. *STXBP1* mutations in early infantile epileptic encephalopathy with suppression-burst pattern. Epilepsia 2010: 51: 2397–2405.
6. Saitsu H, Hoshino H, Kato M et al. Paternal mosaicism of an *STXBP1* mutation in OS. Clin Genet 2010. Epub ahead of print. DOI: 10.1111/j.1399-0004.2010.01575.x.

7. Deprez L, Weckhuysen S, Holmgren P et al. Clinical spectrum of early-onset epileptic encephalopathies associated with *STXBP1* mutations. Neurology 2010: 75: 1159–1165.
8. Hamdan FF, Piton A, Gauthier J et al. De novo *STXBP1* mutations in mental retardation and nonsyndromic epilepsy. Ann Neurol 2009: 65: 748–753.
9. Moretti P, Sahoo T, Hyland K et al. Cerebral folate deficiency with developmental delay, autism, and response to folinic acid. Neurology 2005: 64: 1088–1090.
10. Boone PM, Bacino CA, Shaw CA et al. Detection of clinically relevant exonic copy-number changes by array CGH. Hum Mutat 2010: 31: 1326–1342.
11. Engel J Jr. Report of the ILAE classification core group. Epilepsia 2006: 47: 1558–1568.
12. Lieber MR. The mechanism of double-strand DNA break repair by the nonhomologous DNA end-joining pathway. Annu Rev Biochem 2010: 79: 181–211.
13. Saitsu H, Tohyama J, Kumada T et al. Dominant-negative mutations in alpha-II spectrin cause West syndrome with severe cerebral hypomyelination, spastic quadriplegia, and developmental delay. Am J Hum Genet 2010: 86: 881–891.

Correspondence:
Dr Hirotomo Saitsu
Department of Human Genetics
Yokohama City University Graduate School of Medicine
3-9 Fukuura, Kanazawa-ku
Yokohama 236-0004
Japan
Tel.: +81 45 787 2606
Fax: +81 45 786 5219
e-mail: hsaitsu@yokohama-cu.ac.jp

CLINICAL REPORT

AMERICAN JOURNAL OF medical genetics PART A

Neurodevelopmental Features in 2q23.1 Microdeletion Syndrome: Report of a New Patient With Intractable Seizures and Review of Literature

Mitsuo Motobayashi,[1] Akira Nishimura-Tadaki,[2] Yuji Inaba,[1]* Tomoki Kosho,[3] Satoko Miyatake,[2] Taemi Niimi,[1] Takafumi Nishimura,[1] Keiko Wakui,[3] Yoshimitsu Fukushima,[3] Naomichi Matsumoto,[2] and Kenichi Koike[1]**

[1]Department of Pediatrics, Shinshu University School of Medicine, Matsumoto, Japan

[2]Department of Human Genetics, Yokohama City Graduate School of Medicine, Yokohama, Japan

[3]Department of Medical Genetics, Shinshu University School of Medicine, Matsumoto, Japan

Received 27 June 2011; Accepted 23 December 2011

2q23.1 microdeletion syndrome is a recently characterized chromosomal aberration disorder uncovered through array comparative genomic hybridization (array CGH). Although the cardinal feature is intellectual disability (ID), neurodevelopmental features of the syndrome have not been systematically reviewed. We present a 5-year-old boy with severe psychomotor developmental delay/ID, progressive microcephaly with brain atrophy, growth retardation, and several external anomalies. He manifested intractable epilepsy, effectively treated with combined antiepileptic drug therapy including topiramate. Array CGH demonstrated a de novo interstitial deletion of approximately 1 Mb at 2q23.1–q23.2, involving four genes including *MBD5*. Nineteen patients have been reported to have the syndrome, including present patient. All patients whose data were available had ID, 17 patients (89%) had seizures, and microcephaly was evident in 9 of 18 patients (50%). Deletion sizes ranged from 200 kb to 5.5 Mb, comprising 1–15 genes. *MBD5*, the only gene deleted in all patients, is considered to be responsible for ID and epilepsy. Furthermore, the deletion junction was sequenced for the first time in a patient with the syndrome; and homology of three nucleotides, identified at the distal and proximal breakpoints, suggested that the deletion might have been mediated by recently-delineated genomic rearrangement mechanism Fork Stalling and Template Switching (FoSTeS)/microhomology-mediated break-induced replication (MMBIR).

Key words: 2q23.1 microdeletion syndrome; array CGH; neurological features; epilepsy; *MBD5*; FoSTeS/MMBIR

How to Cite this Article:
Motobayashi M, Nishimura-Tadaki A, Inaba Y, Kosho T, Miyatake S, Niimi T, Nishimura T, Wakui K, Fukushima Y, Matsumoto, N, Koike K. 2012. Neurodevelopmental features in 2q23.1 microdeletion syndrome: Report of a new patient with intractable seizures and review of literature.
Am J Med Genet Part A 158A:861–868.

INTRODUCTION

The 2q23.1 microdeletion syndrome is a recently characterized chromosomal aberration disorder uncovered by array comparative genomic hybridization (array CGH). To date, only 18 patients have been reported to have the syndrome (Table I) [Vissers et al., 2003; Koolen et al., 2004; de Vries et al., 2005; De Gregori et al., 2007; Wagenstaller et al., 2007; Jaillard et al., 2009; Williams et al., 2010; van Bon et al., 2010; Chung et al., 2011]. The cardinal feature is intellectual disability (ID) with pronounced speech delay. Additional features include coarse face, short stature, microcephaly, seizures, and behavioral abnormalities such as stereotypic

Grant sponsor: Research on Intractable Diseases, Ministry of Health, Labour and Welfare; Grant sponsor: Japan Society for the Promotion of Science; Grant sponsor: Japanese Epilepsy Research Foundation; Grant sponsor: Naito Foundation.

Mitsuo Motobayashi and Akira Nishimura-Tadaki have contributed equally to this work.

*Correspondence to:
Yuji Inaba, MD, Department of Pediatrics, Shinshu University School of Medicine, 3-1-1 Asahi, Matsumoto 390-8621, Japan.
E-mail: inabay@shinshu-u.ac.jp
**Correspondence to:
Tomoki Kosho, MD, Department of Medical Genetics, Shinshu University School of Medicine, 3-1-1 Asahi, Matsumoto 390-8621, Japan.
E-mail: ktomoki@shinshu-u.ac.jp

Published online 9 March 2012 in Wiley Online Library (wileyonlinelibrary.com).
DOI 10.1002/ajmg.a.35235

TABLE I. Neurological and Molecular Findings of Our Patient and 18 Previously Reported Patients With Microdeletion Encompassing the 2q23.1 Region

			Deleted region						Seizures					
Patient [reference]	Sex	Array	Start	End	Size (Mb)	Deleted genes	OFC (centile)	MR	Severity	Type	Onset	AEDs	EEG	MRI
Our patient	M	Agilent Oligo 1M	148.8	149.8	0.992	*MBD5, EPC2, KIF5C, LYPD6B*	<3rd (−3.6 SD)	Severe	Severe	CPS	10M	CBZ, ZNS, CLB, TPM	F[#1]	Myelination delay, brain atrophy in F[#1] and T[#2]
1 [Wagenstaller et al., 2007, Patient 27737]	M	Affimetrix SNP 100K	149.0	149.2	0.2	*MBD5*	ND	Severe	Drug resistant	ND	1Y4M	ND	ND	ND
2 [Jaillard et al., 2009, Subject 1]	M	Agilent Oligo 44K	148.8–149.1	149.3–149.4	0.3	*MBD5, EPC2*	<3rd (−3 SD)	Severe	ND	ND	3M	ND	Non-specific	Small cerebellar vermis
3 [van Bon et al., 2010, Patient 8a]	M	Agilent Oligo 244K	148.5	148.9	0.4	*ORC4L, MBD5*	25th	Moderate	—	—	—	—	ND	Normal
4 [van Bon et al., 2010, Patient 8b]	F	Agilent Oligo 244K	148.5	148.9	0.4	*ORC4L, MBD5*	25th	Moderate	ND	ND	10Y	ND	ND	Ventricular asymmetry
5 [van Bon et al., 2010, Patient 7]	M	Agilent Oligo 44K	148.7	149.2	0.5	*MBD5, EPC2*	<3rd	ND	Severe epileptic encephalopathy	GTCS, GTS, AS, Ab	3Y	Multiple	Multiregion	Normal
6 [Williams et al., 2010, Case 1]	F	Agilent Oligo 244K	148.4	149.4	~0.93	*ORC4L, MBD5, EPC2, KIF5C*	<3rd	ND	Well controlled	CPS	8Y	OXC	Mild diffuse encephalopathy changes	Normal
7 [van Bon et al., 2010, Patient 10]	M	Agilent Oligo 244K	148.1	149.2	1.1	*ACVR2A, ORC4L, MBD5, EPC2*	<3rd	Severe	ND	PS, Secondary GS	Newborn	ND	F[#1] and C[#3]	Focal cortical abnormalities in right T[#2]
8 [van Bon et al., 2010, Patient 9]	F	Affymetrix SNP 250K	148.8	150	1.2	*MBD5, EPC2, KIF5C, LYPD6B, LYPD6*	10th	Severe	Drug resistant	ND	10M	ND	Right T[#2] and O[#5]	Wide frontal ventricles and myelination delay
9 [Koolen et al., 2004]	F	BAC 3.6K	145.4–146.7	148.7–151.1	2.0	*PABPCP2, ACVR2A, ORC4L, MBD5, EPC2, KIF5C, LYPD6B*	<3rd (−2 SD)	Severe	ND	GS	12Y	ND	ND	Cortical atrophy
10 [van Bon et al., 2010, Patient 5]	F	Agilent Oligo 244K	148.4	151.1	2.7	*ACVR2A, ORC4L, MBD5, EPC2, KIF5C, LYPD6B, LYPD6, MMADHC, RND3*	50th	Severe	Drug resistant, and died after several seizures	ND	9M	ND	ND	ND
11 [van Bon et al., 2010, Patient 2]	F	Affymetrix SNP 250K	148.7	151.5	2.8	*MBD5, EPC2, KIF5C, LYPD6B, LYPD6, MMADHC, RND3*	10th	ND	ND	ND	3Y10M	ND	ND	Normal

12 [van Bon et al., 2010, Patient 3]	F	Agilent Oligo 244K	148.1	151	2.9	*ACVR2A, ORC4L, MBD5, EPC2, KIF5C, LYPD6B, LYPD6, MMADHC*	50th	Moderate	—	—	—	—	ND	Normal
13 [van Bon et al., 2010, Patient 4]	M	HumanCNV370 CNV-SNP 370K	147.2	150.1	2.9	*ACVR2A, ORC4L, MBD5, EPC2, KIF5C, LYPD6B, LYPD6*	16th	Severe	ND	AS	1Y5M	ND	ND	Thinnng of PCC[#4]
14 [Jaillard et al., 2009, Subject 2]	M	IntegraChips BAC 3K	145.3–146.9	149.3–150.7	2.4–5.4	*PABPCP2, ACVR2A, ORC4L, MBD5, EPC2, KIF5C, LYPD6B, LYPD6, MMADHC*	Median	Severe	ND	ND	3Y	VPA	Normal	Hypoplasia of F[#1]
15 [Williams et al., 2010, Case 2]	F	Agilent Oligo 244K	146.8	150.3	3.51	*PABPCP2, ACVR2A, ORC4L, MBD5, EPC2, KIF5C, LYPD6B, LYPD6, MMADHC*	15th	ND	Well controlled	GTCS	8M	VPA	Light F[#1]	Normal
16 [Chung et al., 2011]	F	Agilent Oligo 105K/244K	148.9	152.9	3.986	*MBD5, EPC2, KIF5C, LYPD6B, LYPD6, MMADHC, RND3, RBM43, NMI, TNFAIP6, RIF1, NEB, ARL5A, CACNB4, STAM2*	<3rd	Moderate, regression at age 6 years	Well controlled	ND	3Y	ND	ND	Normal
17 [van Bon et al., 2010, Patient 6]	M	Cytochip v 3.01 BAC >5K	146.7	151.8	5.2	*PABPCP2, ACVR2A, ORC4L, MBD5, EPC2, KIF5C, LYPD6B, LYPD6, MMADHC, RND3*	<3rd	ND	ND	Ab, Fs	2Y	ND	Normal	Normal
18 [van Bon et al., 2010, Patient 1]	F	Affymetrix SNP 500K	146.6	152.2	5.5	*PABPCP2, ACVR2A, ORC4L, MBD5, EPC2, KIF5C, LYPD6B, LYPD6, MMADHC, RND3, RBM43, NMI, TNFAIP6, RIF1, NEB*	2nd	ND	ND	ND	ND	ND	MD	White matter abnormalities

MR, mental retardation; AEDs, antiepileptic drugs; ND, not described; CPS, complex partial seizure; AS, atonic seizure; Ab, absence seizure; Fs, febrile seizure; GTCS, generalized tonic-clonic seizure; GTS, generalized tonic seizure; GS, generalized seizure; Secondary GS, secondary generalized seizure; PS, partial seizure; CBZ, carbamazepine; ZNS, zonisamide; CLB, clobazam; TPM, topiramate; VPA, valproate; OXC, oxcarbazepine.
F[#1], frontal region; T[#2], temporal region; C[#3], central region; PCC[#4], posterior corpus callosum; O[#5], occipital region.

repetitive behavior, disturbed sleep pattern, and broad-based gait [van Bon et al., 2010].

There have been no reports reviewing neurodevelopmenal features in 2q23.1 microdeletion syndrome. We here present the detailed clinical features and course of a boy with the syndrome who had severe psychomotor developmental delay and ID, progressive microcephaly, and intractable epilepsy that was improved by multi-drug therapy including topiramate (TPM). High-resolution array CGH demonstrated a 992-kb deletion at 2q23.1–q23.2 involving four genes including *MBD5*, and the breakpoint-junction sequencing revealed microhomology of three nucleotides at the distal and proximal breakpoints, suggesting that the deletion might have been mediated by recently delineated genomic rearrangement mechanism Fork Stalling and Template Switching (FoSTeS)/microhomology-mediated break-induced replication (MMBIR).

CLINICAL REPORT

The patient is the third child, with two healthy brothers, of a healthy non-consanguineous 33-year-old mother and 34-year-old father. He was born at 38 weeks of gestation by spontaneous vaginal delivery. His birth weight was 2,960 g (−0.1 SD), length 48.2 cm (−0.2 SD), and OFC 31.5 cm (−1.0 SD). He has suffered from bronchial asthma since infancy. At the age of 10 months, he was referred to our hospital for afebrile clonic seizures involving alternating sides with impaired consciousness. The patient's seizures tended to occur episodically and in clusters. Although he had one episode of status epilepticus for 60 min, most of his seizures were not prolonged. On presentation, his weight, height, and OFC were 9.1 kg (± 0 SD), 71 cm (−0.7 SD), and 42.5 cm (−2.0 SD, Fig. 1a), respectively. He showed psychomotor delay, with a developmental quotient (DQ) of 57 on the Kinder Infant Development Scale (KIDS) [Cheng et al., 2010]. His craniofacial features included brachycephaly, strabismus, a short nose with anteverted nostrils, a short philtrum, macroglossia, a high palate, a bifid uvula, and a submucous cleft palate. Additionally, he had short and curved 5th fingers, a single transverse crease on the right palm, and bilateral undescended testes. Blood levels of lactate and pyruvate and serum levels of thyroid hormones were within normal ranges. Amino acid and organic acid disorders were excluded. A cardiac ultrasonography showed mild supravalvular pulmonary artery stenosis. An interictal EEG showed sporadic spikes in the frontal region during sleep with normal background activity (Fig. 1b). A brain MRI showed no obvious abnormalities and a normal myelination pattern.

The patient's clinical course of epilepsy is shown in Fig. 1c. Carbamazepine (CBZ) was started at the age of 10 months. Seizure frequency and duration decreased, but he began exhibiting stereotypical characteristics of frontal lobe epilepsy (FLE): motion and speech arrested with mild rigidity of the upper limbs and incomplete loss of consciousness for 40–60 sec. Zonisamide (ZNS) resulted in a slight reduction of seizure frequency and clobazam (CLB) controlled his condition for several months, although the seizures restarted with cluster attacks. At the age of 4 years, TPM altered from ZNS reduced his seizure frequency and intensity, disappeared cluster attacks, and shortened (<30 sec) the durations. An interictal EEG showed many paroxysmal discharges with slow wave in the frontal region (Fig. 1d). A brain MRI at the age of 5 years showed delayed myelination and mild brain atrophy (Fig. 1e).

Microcephaly was evident after age 1 (Fig. 1a). The patient could roll over and sit without support at the age of 9 months, walk independently at 21 months, and jump at 4 years. When last examined at the age of 5 years, he weighed 15.2 kg (−1.0 SD) and had a height of 98.3 cm (−2.0 SD), and OFC of 45.3 cm (−3.4 SD). He could produce several words but no sentences. Although he had no regressive psychomotor changes, his DQ as evaluated by KIDS had dropped to 24 from 46 at age 2.

CYTOGENETIC AND MOLECULAR ANALYSIS

G-banded chromosomal analysis (550 bands level) using the patient's peripheral blood leukocytes showed a normal karyotype (46,XY). Array CGH analysis with Agilent 1M array (Agilent Technologies, Inc., Santa Clara, CA) demonstrated a 992-kb heterozygous deletion at 2q23.1–q23.2 (USCS hg18, Mar. 2006, chromosome 2: 148,830,937–149,823,345 bp) (Fig. 2a). The deletion was confirmed with FISH using probes originated from four BACs (RP11-295N18 at 2q22.3, RP11-375H16 at 2q23.1, RP11-1005D13 at 2q23.2, and RP11-714O10 at 2q23.3): RP11-375H16 and RP11-1005D13 were deleted, whereas RP11-295N18 and RP11-714O10 were present (Fig. 2b). Subsequently, the deletion junction was amplified by a long PCR (Fig. 2c; sequences of the primer set are available on request) and its product was directly sequenced (Fig. 2d). Three nucleotides (CTG) were shared by sequences at the proximal breakpoint and the distal breakpoint in normal chromosome 2 (Fig. 2d). FISH analysis using the four BAC probes (data not shown) and the junction PCR on parental samples (Fig. 2c) showed that the deletion had occurred de novo. Therefore, the karyotype was concluded as 46,XY.arr 2q23.1q23.2-(148,830,937–149,823,345) × 1 dn, and he was diagnosed with 2q23.1 microdeletion syndrome involving four genes: *MBD5*, enhancer of polycomb, drosophila, homolog of 2 (*EPC2*), kinesin family member 5C (*KIF5C*), and LY6/PLAUR domain containing 6B (*LYPD6B*).

DISCUSSION

The patient we have described had severe psychomotor developmental delay and ID with progressive microcephaly and intractable seizures improved by multi-drug therapy including TPM. Roughly 1 Mb region at 2q23.1–q23.2, which involved four genes including *MBD5*, was found to be deleted and both the proximal and the distal breakpoints were demonstrated to share microhomology of three nucleotides.

The neurological and molecular cytogenetic findings of 19 patients with the syndrome, including the present patient, are shown in Table I. Microcephaly (OFC < 3rd centile) was evident in 9 of 18 patients (50%), whereas younger patients with OFC > 3rd centile might exhibit microcephaly thereafter as demonstrated in the present patient. Moderate to severe ID was noted in all patients whose data were available. Seventeen patients (89%) had seizures: generalized seizures in five patients, partial seizures in three, and seizures of unspecified nature in nine. Median age of seizure onset

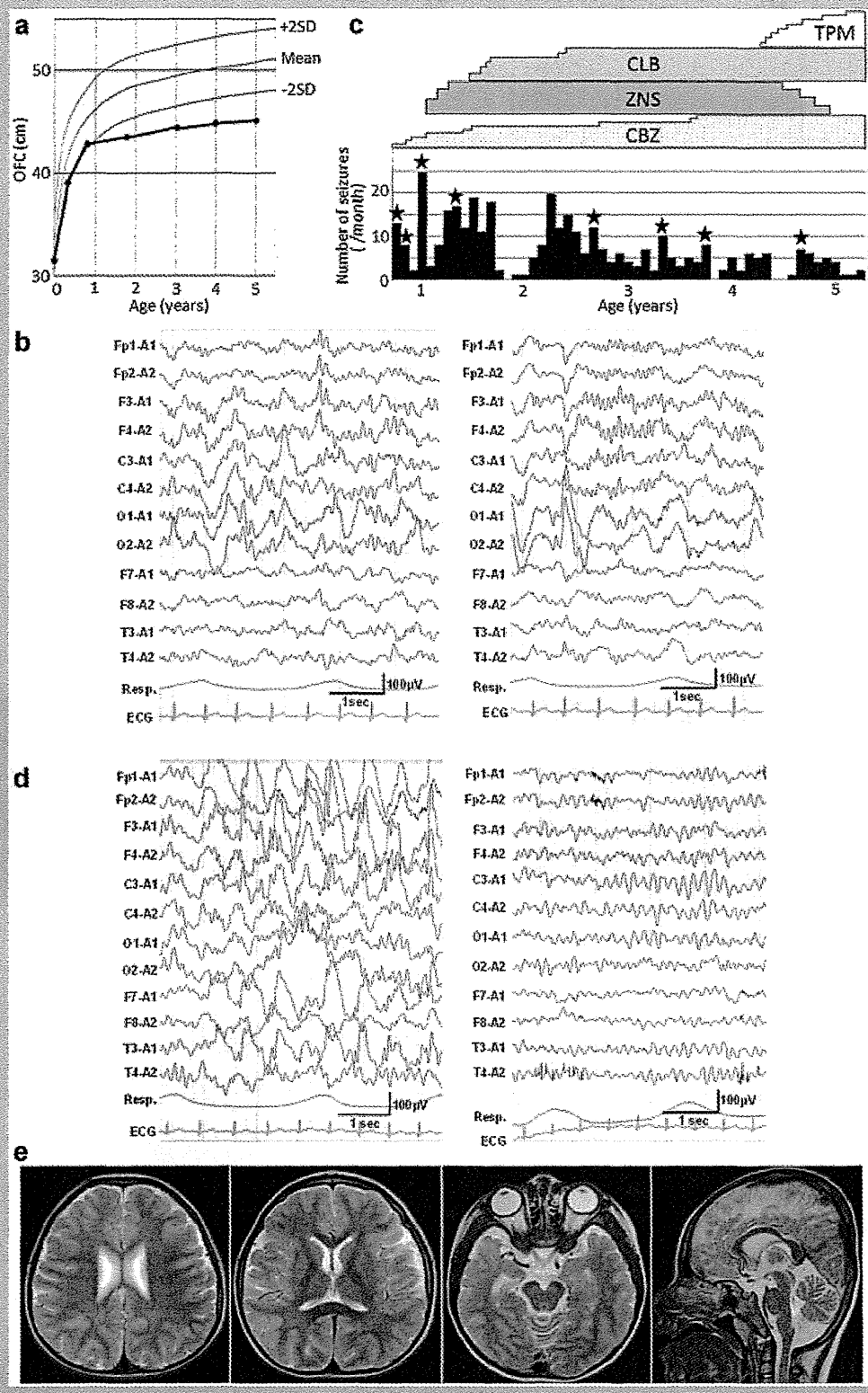

FIG. 1. Clinical findings. a: OFC growth curve. b: An interictal EEG during sleep at age 10 months. Sporadic spikes over the frontal region during sleep records are observed (left). Background activity is consistent with his age (right). c: Therapeutic course of seizures. CBZ, carbamazepine; ZNS, zonisamide; CLB, clobazam; TPM, topiramate. ★ indicates seizures with cluster attacks. d: An interictal EEG at age 4 years. Many paroxysmal discharges including not only sporadic spikes but also slow wave bursts in the bilateral frontal region during sleep are observed (left). A lower frequency theta rhythm in the front-central region during wakefulness is recorded (right). e: Brain MRI at age 5 years. Delayed myelination and mild brain atrophy mainly in the front-temporal lobe are noted.

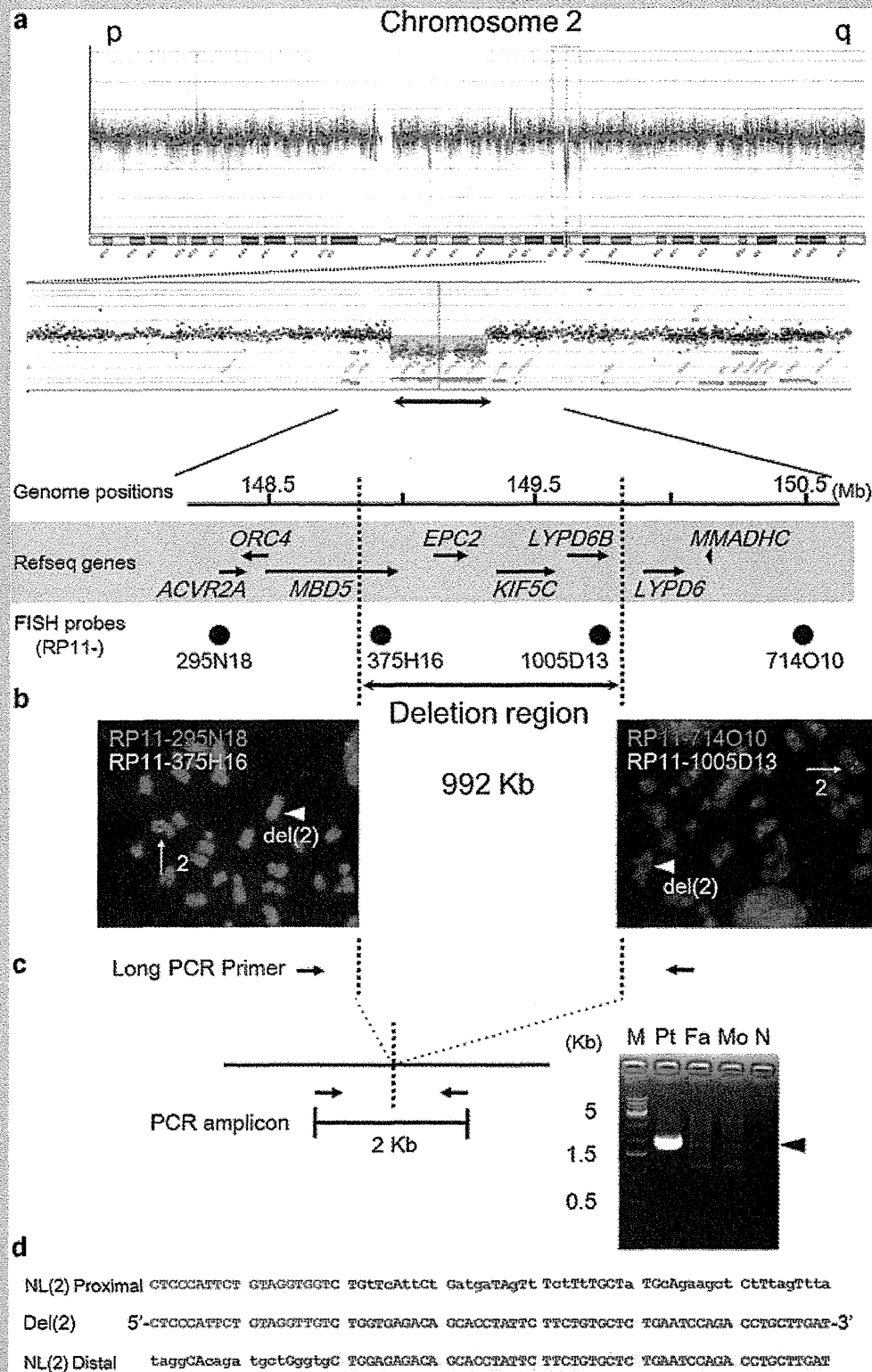

FIG. 2. Cytogenetic and molecular findings. a: High-resolution oligo array [Agilent 1M array] showing the 992 Kb deletion at 2q23.1–q23.2 that contains three Refseq genes [*EPC2*, *KIF5C*, *LYPD6B*] and a disrupted *MBD5*. b: FISH analyses using probes for four BACs [RP11-295N18, RP11-375H16, RP11-1005D13, RP11-714O10]. A normal chromosome 2 [2] is indicated by white arrows and a deleted chromosome 2 [del(2)] is indicated by white arrowheads. Signals for the RP11-375H16 and RP11-1005D13 probes are not detected on deleted chromosome 2. c: Deletion junction PCR showing that an aberrant 2 Kb-PCR amplicon is detected only in the patient [black arrowhead]. M, size markers; Pt, the patient's sample; Fa, the father's sample; Mo, the mother's sample; N, negative control. d: Deletion junction sequence. The normal upper and lower sequences are seen around the proximal [2q23.1] and the distal [2q23.2] deletion breakpoints, respectively. Homologous sequences are indicated by capital letters. The middle sequence is the deletion junction of the patient. NL(2), normal chromosome 2; Del(2), deleted chromosome 2.

was 1 years and 8.5 months (range, neonate to 12 years old). Although the seizures of three patients were well controlled, those of five patients were intractable. In particular, patient 10 began suffering from seizures at the age of 9 months and died at 26 years because of seizures. Patient 5 developed severe epileptic encephalopathy. EEG abnormalities were found in seven of nine patients (78%). The present patient was considered to have FLE with complex partial seizures. His seizures were multi-drug resistant and EEG findings progressively worsened. The effect of CLB was transient, and TPM appeared to be most effective at present to control seizures. MRI abnormalities were detected in 9 of 17 patients (53%) and included cortical atrophy, small vermis, cortical or subcortical lesion, ventricular asymmetry, thinning of the posterior corpus callosum, and delayed myelination. Interestingly, the present patient had no obvious abnormalities during infancy, but later showed brain atrophy and delayed myelination in the front-temporal region at the age of 5 years that were consistent with EEG findings. Considering such a progressive course, careful longitudinal observation of neurodevelopmental features would be necessary for this syndrome. The chromosomal deletion size in the syndrome ranged from 200 kb to 5.5 Mb, but did not seem to correlate with severity of ID, seizures, or MRI abnormalities. Since deleted regions comprised only a part of *MBD5* to 15 genes including *MBD5*, *MBD5* is considered to be responsible for moderate to severe ID and well-controlled to intractable epilepsy.

The deletions in the patients with this syndrome have not been considered to be mediated by NAHR, because the reported deletions did not have common breakpoints [van Bon et al., 2010]. In this study, we sequenced the deletion junction for the first time. The proximal breakpoint was located within a LINE element (LIP3) included in the genomic region of *MBD5*, whereas the distal breakpoint was not located within a LINE element, according to UCSC genome browser. BLAST search found no significant sequence similarity between LIP3 and a sequence around the distal breakpoint in normal chromosome 2. For NAHR to take place, there must be segments of a minimal length sharing extremely high similarity or identity between the low copy repeats, with 10–400 kb in length and >96% sequence identity [Gu et al., 2008]. We, therefore, have concluded the deletion in the present patient not to be mediated by NAHR. Furthermore, we have identified a consensus sequence CTG both at the proximal and the distal breakpoints. This sequence microhomology might have resulted in the deletion in the present patient, via the recently delineated genomic rearrangement mechanism FoSTeS/MMBIR. The mechanism has been reported to mediate genomic rearrangements in Pelizaeus-Merzbacher disease [Lee et al., 2007], Potoki-Lupski microduplication syndrome [Zhang et al., 2009], Smith-Magenis microdeletion syndrome [Zhang et al., 2009], and Charcot-Marie-Tooth disease type 1A duplication/hereditary neuropathies with liability to pressure palsies [Zhang et al., 2009], as well as in 87% of patients with rare pathologic copy number variations [Vissers et al., 2009]. Thorough investigation of breakpoint sequences in the other patients would uncover the etiology of deletions of 2q23.1 microdeletion syndrome.

In conclusion, the present study described detailed neurodevelopmental features including the therapeutic course for intractable epilepsy in a patient with 2q23.1 microdeletion syndrome. Review of neurological and molecular features in previously reported patients demonstrated that *MBD5* would be responsible for ID and epilepsy. Microhomology of three nucleotides, identified at the distal and proximal breakpoints, suggested that the deletion might have been mediated by recently delineated genomic rearrangement mechanism FoSTeS/MMBIR.

ACKNOWLEDGMENTS

The authors are grateful to the patient and his parents. This work was supported by Grants for Research on Intractable Diseases, Ministry of Health, Labour and Welfare (T.K., Y.F., N.M.), a Grant-in-Aid for Scientific Research from Japan Society for the Promotion of Science (JSPS) (N.M.), a Research Grant from Naito Foundation (N.M.), and a Japanese Epilepsy Research Foundation (Y.I.). A.T.-N. is a JSPS fellow.

REFERENCES

Cheng S, Maeda T, Yamagata Z, Tomiwa K, Yamakawa N. 2010. Comparison of factors contributing to developmental attainment of children between 9 and 18 months. J Epidemiol 20:S452–S458.

Chung BH, Stavropoulos J, Marshall CR, Weksberg R, Scherer SW, Yoon G. 2011. 2q23 de novo microdeletion involving the MBD5 gene in a patient with developmental delay, postnatal microcephaly and distinct facial features. Am J Med Genet Part A 155A:424–429.

De Gregori M, Ciccone R, Magini P, Pramparo T, Gimelli S, Messa J, Novara F, Vetro A, Rossi E, Maraschio P, Bonaglia MC, Anichini C, Ferrero GB, Silengo M, Fazzi E, Zatterale A, Fischetto R, Previdere C, Belli S, Turci A, Calabrese G, Bernardi F, Meneghelli E, Riegel M, Rocchi M, Guerneri S, Lalatta F, Zelante L, Romano C, Fichera M, Mattina T, Arrigo G, Zollino M, Giglio S, Lonardo F, Bonfante A, Ferlini A, Cifuentes F, Van Esch H, Backx L, Schinzel A, Vermeesch JR, Zuffardi O. 2007. Cryptic deletions are a common finding in "balanced" reciprocal and complex chromosome rearrangements: A study of 59 patients. J Med Genet 44:750–762.

de Vries BB, Pfundt R, Leisink M, Koolen DA, Vissers LE, Janssen IM, Reijmersdal S, Nillesen WM, Huys EH, Leeuw N, Smeets D, Sistermans EA, Feuth T, van Ravenswaaij-Arts CM, van Kessel AG, Schoenmakers EF, Brunner HG, Veltman JA. 2005. Diagnostic genome profiling in mental retardation. Am J Hum Genet 77:606–616.

Gu W, Zhang F, Lupski JR. 2008. Mechanisms for human genomic rearrangements. Pathogenetics 1:4.

Jaillard S, Dubourg C, Gerard-Blanluet M, Delahaye A, Pasquier L, Dupont C, Henry C, Tabet AC, Lucas J, Aboura A, David V, Benzacken B, Odent S, Pipiras E. 2009. 2q23.1 microdeletion identified by array comparative genomic hybridisation: An emerging phenotype with Angelman-like features?J Med Genet 46:847–855.

Koolen DA, Vissers LE, Nillesen W, Smeets D, van Ravenswaaij CM, Sistermans EA, Veltman JA, de Vries BB. 2004. A novel microdeletion, del(2)(q22.3q23.3) in a mentally retarded patient, detected by array-based comparative genomic hybridization. Clin Genet 65:429–432.

Lee JA, Carvalho CMB, Lupski JR. 2007. A DNA replication mechanism for generating nonrecurrent rearrangements associated with genomic disorders. Cell 131:1235–1247.

van Bon BW, Koolen DA, Brueton L, McMullan D, Lichtenbelt KD, Ades LC, Peters G, Gibson K, Moloney S, Novara F, Pramparo T, Dalla Bernardina B, Zoccante L, Balottin U, Piazza F, Pecile V, Gasparini P, Guerci V, Kets M, Pfundt R, de Brouwer AP, Veltman JA, de Leeuw N,

Wilson M, Antony J, Reitano S, Luciano D, Fichera M, Romano C, Brunner HG, Zuffardi O, de Vries BB. 2010. The 2q23.1 microdeletion syndrome: Clinical and behavioural phenotype. Eur J Hum Genet 18: 163–170.

Vissers LE, de Vries BB, Osoegawa K, Janssen IM, Feuth T, Choy CO, Straatman H, van der Vliet W, Huys EH, van Rijk A, Smeets D, van Ravenswaaij-Arts CM, Knoers NV, van der Burgt I, de Jong PJ, Brunner HG, van Kessel AG, Schoenmakers EF, Veltman JA. 2003. Array-based comparative genomic hybridization for the genomewide detection of submicroscopic chromosomal abnormalities. Am J Hum Genet 73:1261–1270.

Vissers LE, Bhatt SS, Janssen IM, Xia Z, Lalani SR, Pfundt R, Derwinska K, de Vries BB, Gilissen C, Hoischen A, Nesteruk M, Wisniowiecka-Kowalnik B, Smyk M, Brunner HG, Cheung SW, van Kessel AG, Veltman JA, Stankiewicz P. 2009. Rare pathogenic microdeletions and tandem duplications are microhomology-mediated and stimulated by local genomic architecture. Hum Mol Genet 18:3579–3593.

Wagenstaller J, Spranger S, Lorenz-Depiereux B, Kazmierczak B, Nathrath M, Wahl D, Heye B, Glaser D, Liebscher V, Meitinger T, Strom TM. 2007. Copy-number variations measured by single-nucleotide-polymorphism oligonucleotide arrays in patients with mental retardation. Am J Hum Genet 81:768–779.

Williams SR, Mullegama SV, Rosenfeld JA, Dagli AI, Hatchwell E, Allen WP, Williams CA, Elsea SH. 2010. Haploinsufficiency of MBD5 associated with a syndrome involving microcephaly, intellectual disabilities, severe speech impairment, and seizures. Eur J Hum Genet 18:436–441.

Zhang F, Khajavi M, Connolly AM, Towne CF, Batish SD, Lupski JR. 2009. The DNA replication FoSTeS/MMBIR mechanism can generate genomic, genic and exonic complex rearrangements in humans. Nat Genet 41: 849–853.

Molecular Genetics and Metabolism 106 (2012) 43–47

Contents lists available at SciVerse ScienceDirect

Molecular Genetics and Metabolism

journal homepage: www.elsevier.com/locate/ymgme

Contiguous deletion of *SLC6A8* and *BAP31* in a patient with severe dystonia and sensorineural deafness

Hitoshi Osaka [a,*], Atsushi Takagi [a], Yu Tsuyusaki [a], Takahito Wada [a], Mizue Iai [a], Sumimasa Yamashita [a], Hiroko Shimbo [a], Hirotomo Saitsu [c], Gajja S. Salomons [d], Cornelis Jakobs [d], Noriko Aida [b], Shinka Toshihiro [e], Tomiko Kuhara [e], Naomichi Matsumoto [c]

[a] *Division of Neurology, Kanagawa Children's Medical Center, Yokohama, Japan*
[b] *Division of Radiology, Kanagawa Children's Medical Center, Yokohama, Japan*
[c] *Department of Human Genetics, Yokohama City University Graduate School of Medicine, Yokohama, Japan*
[d] *Metabolic Unit, Department of Clinical Chemistry, VU University Medical Center, Amsterdam, The Netherlands*
[e] *Division of Human Genetics, Medical Research Institute, Kanazawa Medical University, Uchinada, Ishikawa, Japan*

ARTICLE INFO

Article history:
Received 1 February 2012
Received in revised form 25 February 2012
Accepted 25 February 2012
Available online 5 March 2012

Keywords:
ATP-binding cassette, sub-family D, member 1 (ABCD1)
B-cell receptor-associated protein (BAP31)
Solute carrier family 6, member 8 (SLC6A8)
Xq28 deletion syndrome

ABSTRACT

We report here a 6-year-old boy exhibiting severe dystonia, profound intellectual and developmental disability with liver disease, and sensorineural deafness. A deficient creatine peak in brain ^{1}H-MR spectroscopy and high ratio of creatine/creatinine concentration in his urine lead us to suspect a creatine transporter (solute carrier family 6, member 8; SLC6A8) deficiency, which was confirmed by the inability to take up creatine into fibroblasts. We found a large ~19 kb deletion encompassing exons 5–13 of *SLC6A8* and exons 5–8 of the B-cell receptor-associated protein (*BAP31*) gene. This case is the first report in which the *SLC6A8* and *BAP31* genes are both deleted. The phenotype of *BAP31* mutations has been reported only as a part of Xq28 deletion syndrome or contiguous ATP-binding cassette, sub-family D, member 1 (*ABCD1*)/DXS1375E (*BAP31*) deletion syndrome [MIM ID #300475], where liver dysfunction and sensorineural deafness have been suggested to be attributed to the loss of function of BAP31. Our case supports the idea that the loss of BAP31 is related to liver dysfunction and hearing loss.

1. Introduction

The creatine (Cr)-creatine phosphate system provides for the storage and fast release of phosphate-bound energy to the muscle and brain. The recent elucidation of congenital genetic diseases supports the vital role of this system in the brain [1]. As such, cerebral Cr deficiency syndrome (CCDS) consists of 3 genetic defects in either L-arginine: glycine amidinotransferase (AGAT), guanidinoacetate methyltransferase (GAMT), or Cr transporter 1 [1]. To date, 9 cases from 4 families with AGAT deficiency (OMIM #612718) and ~40 cases with GAMT-related CCDS (OMIM #601240) have been reported [2]. The solute carrier family 6 (neurotransmitter transporter, creatine), member 8 (*SLC6A8*) maps to Xq28 and encodes Cr transporter 1, which is ubiquitously expressed in human tissues and allows Cr uptake into cells [3]. SLC6A8 deficiency (OMIM #300352) is the most frequent cause of CCDS and reported to constitute ~1–5% of X-linked intellectual disabilities [4–11]. To date, 43 mutations from 44 unrelated families have been reported, including nonsense, missense, and splice-site mutations, single-amino acid deletions, and one large genomic deletion [6,12–15].

The phenotype of SLC6A8 deficiency ranges from mild intellectual disability and speech delay to severe intellectual disability, seizures, and behavioral disorders. The precise pathophysiology of SLC6A8 deficiency remains largely unknown; however, the severe phenotype associated with the large genomic deletion implies that the complete loss of SLC6A8 correlates with severe phenotype. We report here another case of SLC6A8 deficiency syndrome with a large genomic deletion of ~19 kb that encompasses exons 5–13 of *SLC6A8* and exons 5–8 of the B-cell receptor-associated protein (*BAP31*) gene, situating tail-to-tail. As far as we know, this is the first case report with a deletion of both the *SLC6A8* and *BAP31* genes. The phenotype of the *BAP31* mutations has only been reported as part of Xq28 deletion syndrome or contiguous ATP-binding cassette, sub-family D, member 1 (*ABCD1*)/DXS1375E (*BAP31*) deletion syndrome (CADDS; MIM ID #300475) [16]. Patients with CADDS manifest with leukodystrophy due to an *ABCD1* mutation. Moreover, liver dysfunction and sensorineural deafness reportedly accompany the adrenoleukodystrophy (ALD) phenotype, implicating its attribution to the loss of function of BAP31. Our case supports the relationship between the loss of BAP31 and liver dysfunction and hearing loss.

* Corresponding author at: Division of Neurology, Clinical Research Institute, Kanagawa Children's Medical Center, Mutsukawa 2-138-4, Minami-ku, Yokohama, 232-8555, Japan. Fax: +81 45 721 332.
E-mail address: hosaka@kcmc.jp (H. Osaka).

1096-7192/$ – see front matter © 2012 Elsevier Inc. All rights reserved.
doi:10.1016/j.ymgme.2012.02.018

2. Materials and methods

2.1. Patient

This 6-year-old boy is the only child of his nonconsanguineous Japanese parents. He was born with a body weight of 2478 g without asphyxia at 37 weeks. He was noted to have poor weight gain at ~2 months. He exhibited hypertonus and athetosis at 4 months, and was referred to our neurology division for evaluation at 8 months. At first evaluation, he showed failure to thrive with a body weight of 6.0 kg (−2.7 SD) and height of 60.0 cm (−4.4 SD).

He showed no dysmorphic features and behavioral problems. He could not hold his head or follow an object with his eyes. His muscle tone was hypertonic and all extremities displayed exaggerated tendon reflexes and bilateral extensor plantar responses. Dystonia was also evident in his upper and lower extremities. Routine laboratory examinations revealed mild elevations of aminotransferase/alanine aminotransferase (AST/ALT) of ~100 IU/mL; however, there were no biochemical abnormalities in the levels of serum ammonia, lactate, and pyruvate, very long chain fatty acids, or arylsulfatase A. Nerve conduction velocities and electromyographic studies were all normal. No waves were identified by auditory evoked brain responses, even at a maximum stimulation intensity of 115 dB. Magnetic resonance imaging (MRI) revealed abnormal increased signals in the globus pallidi on T2-weighted images (Fig. 1A, upper left). Myelination delay, a decrease in the volume of cerebral white matter, and a very thin corpus callosum were also observed (Fig. 1A, lower left). At 4 years of age, he was admitted to our hospital due to status epileptics with generalized tonic–clonic seizures lasting 1 h, which were controlled by intravenous diazepam. Electroencephalography showed frequent spikes and slow waves in central and mid-temporal areas. He was initiated with phenobarbital and no seizures have been noticed since then. MRI revealed the completion of myelination, persistent signal abnormalities in the globus pallidi, and the progression of cerebellar vermian atrophy (Fig. 1A, right panels). A deficient Cr peak in ^{1}H-magnetic resonance spectroscopy (MRS) (Fig. 1B) and high ratio of creatine/creatinine concentration in urine 4.73 mmol/mmol (normal range; 0.0075-1.51) led us to suspect SLC6A8 deficiency [17]. Now he is still very small and showing severe dystonia at 6 years of ages. He cannot hold his head and does not pursuit object. During upper respiratory infections, he showed increased levels of AST/ALT >10,000 IU/mL without cholestasis. These values returned to his baseline levels without any therapy after a few weeks.

2.2. Cr uptake in fibroblasts

Cr uptake was measured in total cell lysates in triplicate using gas chromatography–mass spectrometry with stable isotope-labeled Cr as the internal standard, as described by Rosenberg et al. [18]. Briefly, fibroblasts from the patient were cultured for 24 h in medium (HAM/F10 supplemented with 10% fetal bovine serum, penicillin, and streptavidin) that contained physiological levels of Cr (25 mM). Cr was added to the medium and obtains final concentrations of 25 and 500 mM [12].

2.3. Genomic DNA sequencing, RT-PCR, and sequencing

Genomic DNA was prepared from the patient's white blood cells using the Wizard Genomic DNA Purification Kit (Promega, Madison, WI, USA). PCR of all exons and exon–intron boundaries of the *SLC6A8* gene was performed as previously described [10]. Subsequent sequencing analyses of the PCR fragments were performed with specific primers using the Ex Taq PCR Kit (version 1.0; Takara, Shiga, Japan) according to the manufacturer's instructions (Supplementary Table). PCR buffers were selected from the GC I, GC II, and EX buffers (Takara) (Supplementary Table). Total RNA was extracted from leukocytes using the TRIzol reagent and reverse transcribed with Prime Script Reverse Transcriptase (Takara, Shiga, Japan) using oligo(dT) primers. RT-PCR was performed using primers that covered from exon 2 to exon 13 according to the manufacturer's instructions (Supplementary Table). The PCR fragments were sequenced using the Big Dye Terminators Cycle Sequencing Kit (v1.1; Applied Biosystems, Foster City, CA, USA).

2.4. Western blotting

Fibroblasts (~3.0×10^{5} cells) were harvested and lysed with 300 μL of SDS lysis buffer (100 mM Tris–HCl (pH 6.8), 2% SDS, 100 mM DTT, 20% sucrose). After boiling for 5 min, aliquots were

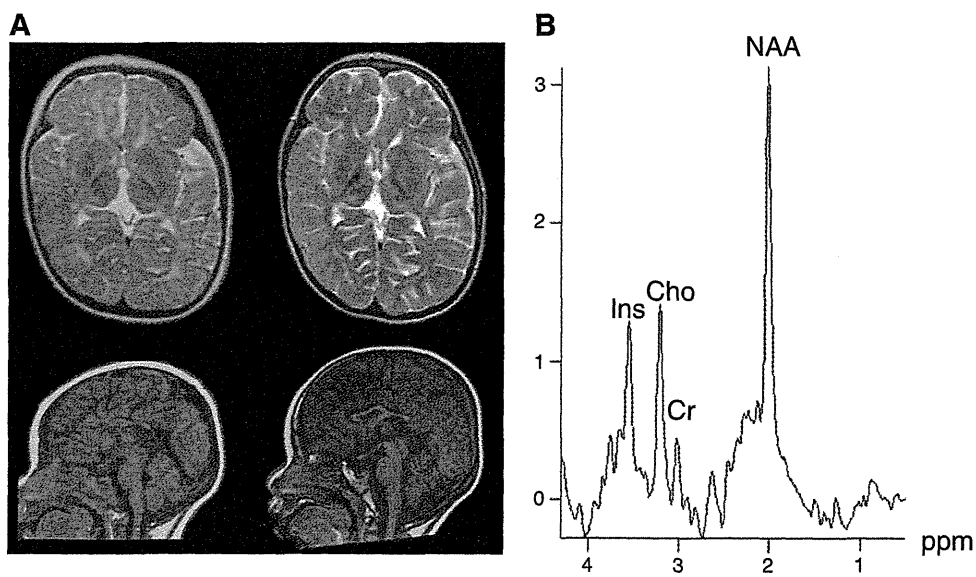

Fig. 1. MRI and MRS. T2-weighted axial image at 8 months shows an abnormal increased signal in the globus pallidi, myelination delay, and a decreased volume of cerebral white matter (A; upper left). T1-weighted sagittal image demonstrating a very thin corpus callosum (A; lower left). T2-weighted axial image (A; upper right) and T1-weighted sagittal image (A; lower right) at 4 years show persistent high signals in the globus pallidi, thin corpus callosum, and progression of cerebellar vermian atrophy. ^{1}H-MRS from the left basal ganglia at 4 years (B). MRS at 4 years shows a very low peak of Cr at 3.0 ppm (arrowhead).

analyzed by western blotting using the XV PANTERA Gel System (DRC, Tokyo, Japan). Detection was performed using the ECL-Advance System (GE Healthcare, Buckinghamshire, UK). The primary antibody was rat monoclonal anti-BAP31 antibody (1:1000, sc-56007; Santa Cruz Biotechnology, Santa Cruz, CA, USA). The secondary antibody was goat anti-rat IgG-HRP conjugate (1:2000, sc-2006; Santa Cruz Biotechnology, Santa Cruz, CA, USA).

3. Results

3.1. Cr uptake in fibroblasts

The uptake of Cr in fibroblasts from the patient was almost undetectable (0.19 pmol Cr/μg protein) when incubated at a physiological Cr concentration (25 μmol/L) (controls: n = 13, 27.8 ± 5.6 pmol Cr/μg protein; Cr transporter deficiency patients: n = 12, 0.58 ± 1.03 pmol Cr/μg protein) [12].

3.2. PCR, RT-PCR analysis, and sequencing

As MRI and the Cr uptake test strongly suggested an SLC6A8 deficiency, we analyzed *SLC6A8*. We could not obtain PCR products from exons 5–13 of *SLC6A8* in the patient. As we could amplify DNA from various exons of *ABCD1*, we performed a long-range PCR using various primers that were spaced between *SLC6A8* and *ABCD1*. We obtained an ~500 bp PCR product using primers at intron 4 of *SLC6A8* and the other one situated ~20 kb-telomeric. Sequencing this fragment revealed breakpoints at intron 4 of *SLC6A8* and intron 4 of *BAP31*, which are situated tail-to-tail (Figs. 2A, B). The deletion encompasses ~19 kb and involves exons 5–13 of *SLC6A8* and exons 5–8 of *BAP31* (Figs. 2B, C). Next, we analyzed the effects of this deletion on the transcript level of both genes. RT-PCR between exon 2 and 3′-UTR of *SLC6A8* revealed an aberrant *SLC6A8* transcript in which intron 4 was incorporated, resulting in a truncated protein of 391 amino acids (a.a.), much shorter than the wild-type protein (635 a.a.) (Fig. 3A). Similarly, we detected *BAP31* mRNA in which intron 4 of *BAP31* remained in the transcript. The deduced sequence predicted a 114-a.a. protein that is much shorter than wild-type *BAP31* (isoform a, 313 a.a.; isoform b, 246 a.a.)(Fig. 3B). Primers flanking the deletion successfully amplified a 507-bp product only from the patient among family members, indicating that the deletion occurred de novo (Fig. 3C).

3.3. Western blotting

We detected BAP31 protein of ~28 kDa in normal control fibroblasts. However, we could not detect a signal for BAP31 in fibroblasts from the patient, even at ~12 kDa, deduced from the possible mRNA predicted size, indicating either nonsense-mediated decay of the aberrant mRNA or the short half-life of truncated BAP31 (Fig. 3D).

4. Discussion

The reported phenotype of Cr transporter deficiency consists of intellectual disability, language delay, seizures, and autistic behavior [13]. Although >40 mutations of *SLC6A8* have been reported, a clear geno-phenotypic correlation has not been established. Two cases, one case with a large genomic deletion of exons 8–13 of *SLC6A8* and another with a deletion of the complete coding region of *SLC6A8*, showed severe developmental delay, seizures, failure to thrive, and dystonia [15]. Cellular Cr uptake was almost completely lost in these two patients. Our case is the third patient to be described with a large *SLC6A8* deletion, and also showed similar severe developmental delay, failure to thrive, and dystonia. A large genomic deletion of exons 8–13 of *SLC6A8* is suggestive for a loss-of-function of SLC6A8 and, indeed, Cr uptake was disrupted in our patient. The symptoms of these three cases are more severe than those of patients with single nucleotide mutations, and it appears that the complete loss of

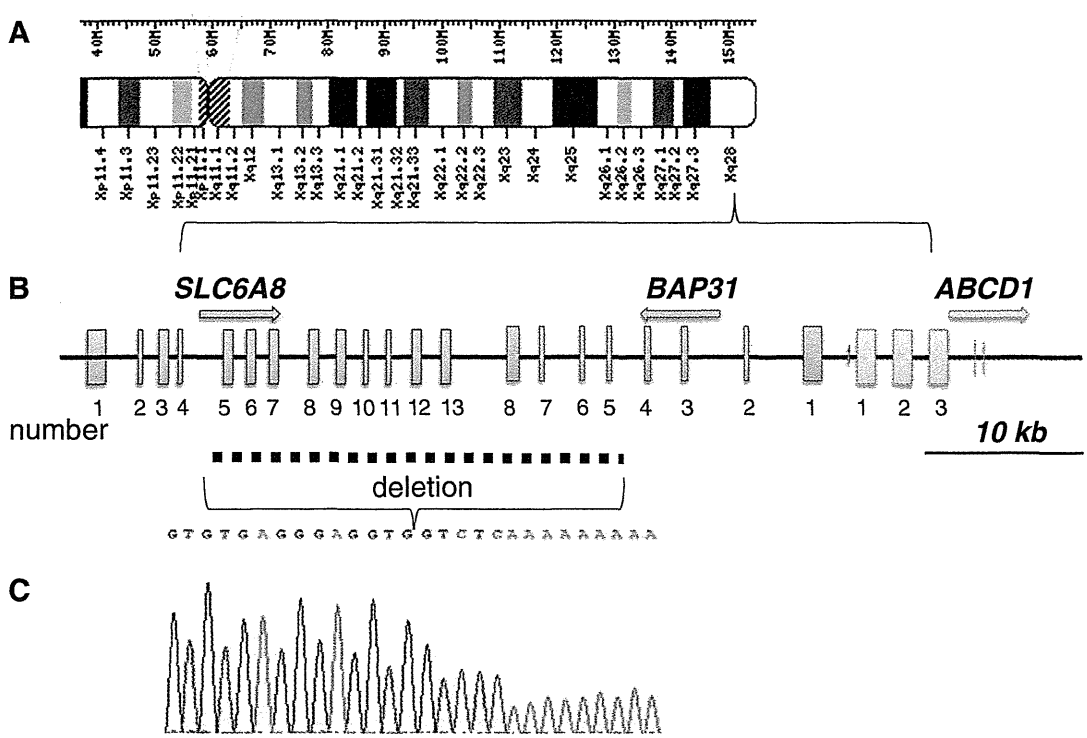

Fig. 2. 19-kb deletion involving *SLC6A8* and *BAP31*.(A) Position of the *SLC6A8* and *BAP31* genes on Chr. Xq28.(B) Position of *SLC6A8*, *BAP31*, and *ABCD1*. *BAP31* and *SLC6A8* are tail-to-tail orientation.(C) Sequence chromatogram around the conjugation point of the two breakpoints. Intron 4 of *SLC6A8* and intron 4 of *BAP31* are joined.

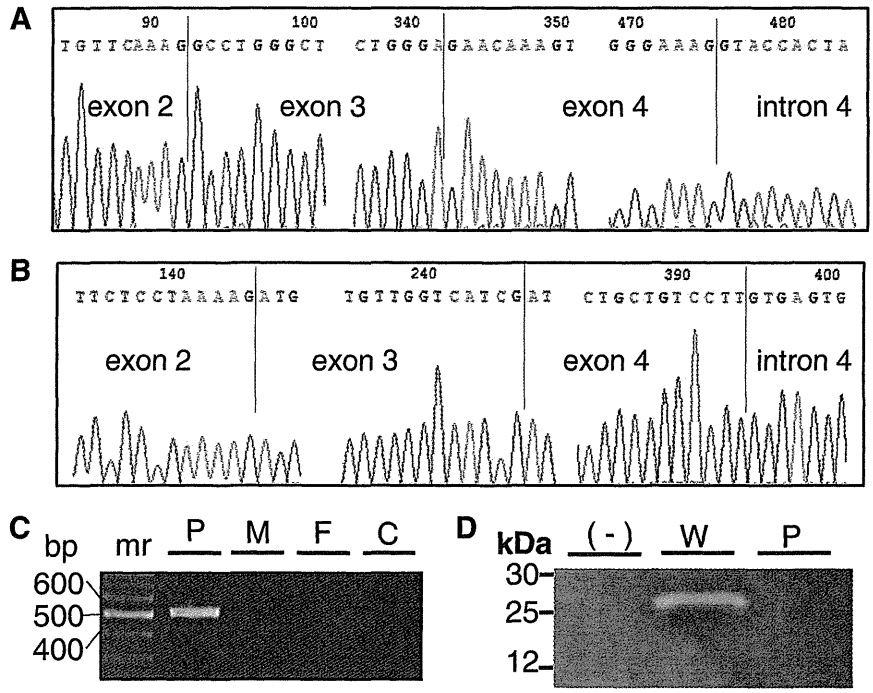

Fig. 3. RT-PCR and sequencing of *SLC6A8* and *BAP31*. RT-PCR with primers at exon 2 and 3′-UTR of *SLC6A8* indicates the transcript involves intron 4 (A). RT-PCR between exon 2 and intron 4 of *BAP31* revealed the transcript contains intron 4 (B). Breakpoint-specific PCR analysis of the patient's family (C). Primers flanking the deletion successfully amplified a 507-bp product from the patient, indicating the deletion occurred *de novo*. P, patient; M, mother; F, father; C, normal control; mr, markers. Western blotting from fibroblasts from wild-type (W) and patient (P) (D). The primary antibody was rat monoclonal anti-BAP31 (1:1000) and the secondary antibody was goat anti-rat IgG-HRP conjugate (1:2000, sc-2006). The band of ~28 kDa shown in the wild-type is unseen in the patient.

transporter function leads to severe neurological dysfunction. As for the two previously reported cases, the breakpoints have not been elucidated and therefore, we cannot exclude the possibility that the severe phenotype of these three cases is influenced by BAP31.

We discovered a large ~19-kb deletion that encompassed exons 5–13 of *SLC6A8* and exons 5–8 of *BAP31*. As far as we know, this report is the first case presentation in which *SLC6A8* and *BAP31* are both mutated. Phenotype of the *BAP31* mutations has been only reported as a part of Xq28 deletion syndrome or (CADDS) [MIM ID #300475]. Since deletion causes complete loss of *ABCD1*, these patients develop cerebral demyelination at more early age compared to classical ALD. Moreover, patients with CADDS also showed liver disease and sensorineural deafness. These two clinical symptoms have been suggested to originate from the loss of BAP31 function. However, other than these 3 cases with CADDS, mutations of *BAP31* have not been reported. Our case, carrying a deletion of *SLC6A8* and *BAP31*, also displayed an overlapping phenotype with CADDS, i.e., liver disease and sensorineural deafness. Our case strengthens the idea that the loss of BAP31 is related to liver disease and sensorineural deafness. Sequencing of *BAP31* in patients with X-linked sensorineural deafness may help to clarify this further.

Recently, BAP31 was shown to be a component of the quality control system of the endoplasmic reticulum (ER). By receiving apoptotic signals from mitochondria, BAP31 is involved in the activation of procaspase-8. Thus, BAP31 is emerging as critical component of ER stress signaling between mitochondria and the ER [19]. Our present case had increased levels of AST/ALT during an infection that induced ER stress; therefore, it is possible that dysfunction of mitochondrial-ER signaling is involved in the recurrent liver dysfunction observed during infection in our case. Wolfram syndrome-1 is a severe autosomal recessive neurodegerative disease characterized by diabetes mellitus, optic atrophy, diabetes insipidus, and deafness (WFS1; OMIM #222300). Recently, WFS1 was shown to negatively regulate a key transcription factor involved in ER stress signaling, activating transcription factor 6α (ATF6α), through the ubiquitin-proteasome pathway[20]. It is tempting to speculate the defect in ER stress signaling accounts for association of BAP31 to deafness and liver disease.

Supplementary materials related to this article can be found online at doi:10.1016/j.ymgme.2012.02.018.

Conflict of interest statement

We have no conflict of interest to disclose.

Acknowledgments

This work was supported by research grants from the Ministry of Health, Labour and Welfare (H.O., T.W., and N. M), the Japan Science and Technology Agency (N. M), the Strategic Research Program for Brain Sciences (N. M), a Grant-in-Aid for Scientific Research on Innovative Areas-(Foundation of Synapse and Neurocircuit Pathology)-from the Ministry of Education, Culture, Sports, Science and Technology of Japan (N. M), and a Grant-in-Aid for Scientific Research from Japan Society for the Promotion of Science (H.O., N. M).

References

[1] S. Stockler, P.W. Schutz, G.S. Salomons, Cerebral creatine deficiency syndromes: clinical aspects, treatment and pathophysiology, Subcell. Biochem. 46 (2007) 149–166.
[2] N. Longo, O. Ardon, R. Vanzo, E. Schwartz, M. Pasquali, Disorders of creatine transport and metabolism, Am. J. Med. Genet. C Semin. Med. Genet. 157 (2011) 72–78.
[3] P. Gregor, S.R. Nash, M.G. Caron, M.F. Seldin, S.T. Warren, Assignment of the creatine transporter gene (SLC6A8) to human chromosome Xq28 telomeric to G6PD, Genomics 25 (1995) 332–333.
[4] E.H. Rosenberg, L.S. Almeida, T. Kleefstra, R.S. deGrauw, H.G. Yntema, N. Bahi, C. Moraine, H.H. Ropers, J.P. Fryns, T.J. deGrauw, C. Jakobs, G.S. Salomons, High prevalence of SLC6A8 deficiency in X-linked mental retardation, Am. J. Hum. Genet. 75 (2004) 97–105.

[5] A. Newmeyer, K.M. Cecil, M. Schapiro, J.F. Clark, T.J. Degrauw, Incidence of brain creatine transporter deficiency in males with developmental delay referred for brain magnetic resonance imaging, J. Dev. Behav. Pediatr. 26 (2005) 276–282.
[6] A.J. Clark, E.H. Rosenberg, L.S. Almeida, T.C. Wood, C. Jakobs, R.E. Stevenson, C.E. Schwartz, G.S. Salomons, X-linked creatine transporter (SLC6A8) mutations in about 1% of males with mental retardation of unknown etiology, Hum. Genet. 119 (2006) 604–610.
[7] L. Lion-Francois, D. Cheillan, G. Pitelet, C. Acquaviva-Bourdain, G. Bussy, F. Cotton, L. Guibaud, D. Gerard, C. Rivier, C. Vianey-Saban, C. Jakobs, G.S. Salomons, V. des Portes, High frequency of creatine deficiency syndromes in patients with unexplained mental retardation, Neurology 67 (2006) 1713–1714.
[8] A. Arias, M. Corbella, C. Fons, A. Sempere, J. Garcia-Villoria, A. Ormazabal, P. Poo, M. Pineda, M.A. Vilaseca, J. Campistol, P. Briones, T. Pampols, G.S. Salomons, A. Ribes, R. Artuch, Creatine transporter deficiency: prevalence among patients with mental retardation and pitfalls in metabolite screening, Clin. Biochem. 40 (2007) 1328–1331.
[9] O.T. Betsalel, J.M. van de Kamp, C. Martinez-Munoz, E.H. Rosenberg, A.P. de Brouwer, P.J. Pouwels, M.S. van der Knaap, G.M. Mancini, C. Jakobs, B.C. Hamel, G.S. Salomons, Detection of low-level somatic and germline mosaicism by denaturing high-performance liquid chromatography in a EURO-MRX family with SLC6A8 deficiency, Neurogenetics 9 (2008) 183–190.
[10] H. Puusepp, K. Kall, G.S. Salomons, I. Talvik, M. Mannamaa, R. Rein, C. Jakobs, K. Ounap, The screening of SLC6A8 deficiency among Estonian families with X-linked mental retardation, J. Inherit. Metab. Dis. (2009).
[11] O. Ardon, C. Amat di San Filippo, G.S. Salomons, N. Longo, Creatine transporter deficiency in two half-brothers, Am. J. Med. Genet. A 152A (2010) 1979–1983.
[12] E.H. Rosenberg, C. Martinez Munoz, O.T. Betsalel, S.J. van Dooren, M. Fernandez, C. Jakobs, T.J. deGrauw, T. Kleefstra, C.E. Schwartz, G.S. Salomons, Functional characterization of missense variants in the creatine transporter gene (SLC6A8): improved diagnostic application, Hum. Mutat. 28 (2007) 890–896.
[13] G.S. Salomons, S.J. van Dooren, N.M. Verhoeven, D. Marsden, C. Schwartz, K.M. Cecil, T.J. DeGrauw, C. Jakobs, X-linked creatine transporter defect: an overview, J. Inherit. Metab. Dis. 26 (2003) 309–318.
[14] O.T. Betsalel, E.H. Rosenberg, L.S. Almeida, T. Kleefstra, C.E. Schwartz, V. Valayannopoulos, O. Abdul-Rahman, N. Poplawski, L. Vilarinho, P. Wolf, J.T. den Dunnen, C. Jakobs, G.S. Salomons, Characterization of novel SLC6A8 variants with the use of splice-site analysis tools and implementation of a newly developed LOVD database, Eur. J. Hum. Genet. 19 (2011) 56–63.
[15] I.A. Anselm, F.S. Alkuraya, G.S. Salomons, C. Jakobs, A.B. Fulton, M. Mazumdar, M. Rivkin, R. Frye, T.Y. Poussaint, D. Marsden, X-linked creatine transporter defect: a report on two unrelated boys with a severe clinical phenotype, J. Inherit. Metab. Dis. 29 (2006) 214–219.
[16] D. Corzo, W. Gibson, K. Johnson, G. Mitchell, G. LePage, G.F. Cox, R. Casey, C. Zeiss, H. Tyson, G.R. Cutting, G.V. Raymond, K.D. Smith, P.A. Watkins, A.B. Moser, H.W. Moser, S.J. Steinberg, Contiguous deletion of the X-linked adrenoleukodystrophy gene (ABCD1) and DXS1357E: a novel neonatal phenotype similar to peroxisomal biogenesis disorders, Am. J. Hum. Genet. 70 (2002) 1520–1531.
[17] C. Valongo, M.L. Cardoso, P. Domingues, L. Almeida, N. Verhoeven, G. Salomons, C. Jakobs, L. Vilarinho, Age related reference values for urine creatine and guanidinoacetic acid concentration in children and adolescents by gas chromatography-mass spectrometry, Clin. Chim. Acta 348 (2004) 155–161.
[18] G.S. Salomons, S.J. van Dooren, N.M. Verhoeven, K.M. Cecil, W.S. Ball, T.J. Degrauw, C. Jakobs, X-linked creatine-transporter gene (SLC6A8) defect: a new creatine-deficiency syndrome, Am. J. Hum. Genet. 68 (2001) 1497–1500.
[19] R. Iwasawa, A.L. Mahul-Mellier, C. Datler, E. Pazarentzos, S. Grimm, Fis1 and Bap31 bridge the mitochondria-ER interface to establish a platform for apoptosis induction, EMBO J. 30 (2011) 556–568.
[20] S.G. Fonseca, S. Ishigaki, C.M. Oslowski, S. Lu, K.L. Lipson, R. Ghosh, E. Hayashi, H. Ishihara, Y. Oka, M.A. Permutt, F. Urano, Wolfram syndrome 1 gene negatively regulates ER stress signaling in rodent and human cells, J. Clin. Invest. 120 (2010) 744–755.

nature genetics

Mutations affecting components of the SWI/SNF complex cause Coffin-Siris syndrome

Yoshinori Tsurusaki[1], Nobuhiko Okamoto[2], Hirofumi Ohashi[3], Tomoki Kosho[4], Yoko Imai[5], Yumiko Hibi-Ko[5], Tadashi Kaname[6], Kenji Naritomi[6], Hiroshi Kawame[7,8], Keiko Wakui[4], Yoshimitsu Fukushima[4], Tomomi Homma[9], Mitsuhiro Kato[10], Yoko Hiraki[11], Takanori Yamagata[12], Shoji Yano[13], Seiji Mizuno[14], Satoru Sakazume[15], Takuma Ishii[15,16], Toshiro Nagai[15], Masaaki Shiina[17], Kazuhiro Ogata[17], Tohru Ohta[18], Norio Niikawa[18], Satoko Miyatake[1], Ippei Okada[1], Takeshi Mizuguchi[1], Hiroshi Doi[1], Hirotomo Saitsu[1], Noriko Miyake[1] & Naomichi Matsumoto[1]

By exome sequencing, we found *de novo SMARCB1* mutations in two of five individuals with typical Coffin-Siris syndrome (CSS), a rare autosomal dominant anomaly syndrome. As *SMARCB1* encodes a subunit of the SWItch/Sucrose NonFermenting (SWI/SNF) complex, we screened 15 other genes encoding subunits of this complex in 23 individuals with CSS. Twenty affected individuals (87%) each had a germline mutation in one of six SWI/SNF subunit genes, including *SMARCB1*, *SMARCA4*, *SMARCA2*, *SMARCE1*, *ARID1A* and *ARID1B*.

Chromatin remodeling factors regulate the gene accessibility and expression by dynamic alteration of chromatin structure. SWI/SNF complexes have important roles in lineage specification, maintenance of stem cell pluripotency and tumorigenesis[1–5]. These complexes are composed of evolutionarily conserved core subunits and variant subunits. Brahma-associated factor (BAF) and Polybromo BAF (PBAF) complexes constitute two major subclasses[1–5]. It has been suggested that the BAF complex is similar to the yeast SWI/SNF complex and that the PBAF complex is more like the chromatin remodelling complex (RSC) in yeast, which is required for cell cycle progression through mitosis[6]. However, several subunits that are common to both BAF and PBAF complexes are predicted to be related to the regulation of lineage- and tissue-specific gene expression[2].

Coffin-Siris syndrome (*MIM 135900*) is a rare congenital anomaly syndrome characterized by growth deficiency, intellectual disability, microcephaly, coarse facial features and hypoplastic nail of the fifth finger and/or toe (**Fig. 1** and **Supplementary Table 1**)[7]. The majority of affected individuals represent sporadic cases, which is compatible with an autosomal dominant inheritance mechanism. The genetic cause for this syndrome has not been elucidated.

To identify the genetic basis of CSS, we performed whole-exome sequencing of five typical affected individuals (**Supplementary Methods**). Taking into account our model that assumes that an abnormality in a causal gene would be shared in two or more subjects, 51 variants were identified as candidates (**Supplementary Table 2**). All the variants were also examined by Sanger sequencing of PCR products amplified using genomic DNA from the five affected individuals and their parents. Nine variants were found to be false positives, 40 were inherited from either the father or mother, and 2 *de novo* heterozygous mutations of *SMARCB1* were found in 2 affected individuals (c.1130G>A (p.Arg377His) and c.1091_1093del AGA (p.Lys364del)) (**Table 1**, **Supplementary Fig. 1** and **Supplementary Methods**). Two *de novo* coding-sequence mutations occurring within a specific gene is an extremely unlikely event[8], supporting the idea that *SMARCB1* is a causative gene in CSS. Next, we screened *SMARCB1* in 23 individuals with CSS by high-resolution melting analysis[9] and identified the mutation encoding the p.Lys364del alteration in two additional individuals, including one of Arab descent (subject 22) (**Table 1** and **Supplementary Fig. 1**). As the mutation detection rate was relatively low (4 of 23, only 17.4%), we screened 15 additional genes encoding other SWI/SNF subunits (**Supplementary Table 3**). Unexpectedly, four other subunits, *SMARCA4* (also known as *BRG1*), *SMARCE1*, *ARID1A* and *ARID1B* were also found to be mutated (**Table 1** and **Supplementary Figs. 2–5**). In subject 10, a, c.2144C>T mutation in *ARID1B* (encoding p.Pro715Leu) was found in addition to the c.5632delG mutation in *ARID1B*. RT-PCR products that were amplified from total RNA from this subject's lymphoblastoid cells were cloned into the pCR4-TOPO vector. The two mutations were present on different alleles, according to sequencing of clones containing each allele (data not shown). As the c.5632delG mutation is

[1]Department of Human Genetics, Yokohama City University Graduate School of Medicine, Yokohama, Japan. [2]Division of Medical Genetics, Osaka Medical Center and Research Institute for Maternal and Child Health, Izumi, Japan. [3]Division of Medical Genetics, Saitama Children's Medical Center, Iwatsuki, Japan. [4]Department of Medical Genetics, Shinshu University School of Medicine, Matsumoto, Japan. [5]Division of Pediatrics, Japanese Red Cross Medical Center, Tokyo, Japan. [6]Department of Medical Genetics, University of the Ryukyus Faculty of Medicine, Okinawa, Japan. [7]Department of Genetic Counseling, Graduate School of Humanities and Sciences, Ochanomizu University, Tokyo, Japan. [8]Division of Medical Genetics, Nagano Children's Hospital, Azumino, Japan. [9]Division of Pediatrics, Yamagata Prefectural and Sakata Municipal Hospital Organization, Nihonkai General Hospital, Sakata, Japan. [10]Department of Pediatrics, Yamagata University Faculty of Medicine, Yamagata, Japan. [11]Hiroshima Municipal Center for Child Health and Development, Hiroshima, Japan. [12]Department of Pediatrics, Jichi Medical University, Tochigi, Japan. [13]Genetics Division, Department of Pediatrics, Los Angeles County and University of Southern California Medical Center, Keck School of Medicine, University of Southern California, Los Angeles, California, USA. [14]Department of Pediatrics, Central Hospital, Aichi Human Service Center, Kasugai, Japan. [15]Department of Pediatrics, Koshigaya Hospital, Dokkyo University School of Medicine, Koshigaya, Japan. [16]Nakagawa-No-Sato, Hospital for the Disabled, Saitama, Japan. [17]Department of Biochemistry, Yokohama City University Graduate School of Medicine, Yokohama, Japan. [18]Research Institute of Personalized Health Sciences, Health Sciences University of Hokkaido, Ishikari-Tobetsu, Japan. Correspondence should be addressed to N. Matsumoto (naomat@yokohama-cu.ac.jp) or N. Miyake (nmiyake@yokohama-cu.ac.jp).

Received 29 September 2011; accepted 10 February 2012; published online 18 March 2012; doi:10.1038/ng.2219

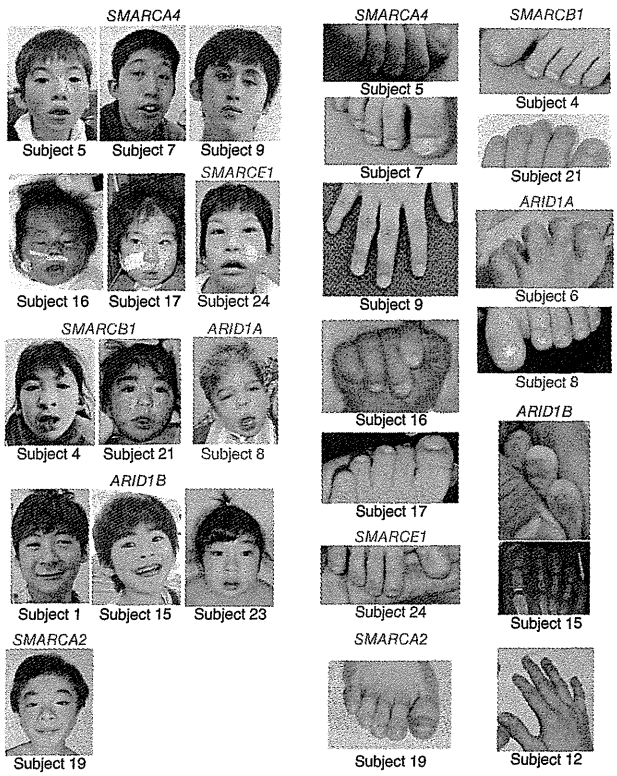

Figure 1 Photographs of individuals with Coffin-Siris syndrome. The faces (left) and hypoplastic-to-absent nail of the fifth finger or toe (right) of affected individuals are shown with the color-coded names of the corresponding mutated genes. The green arrow indicates the absence of the distal phalanx in the fifth toe. No obvious hypoplastic nails were observed in subjects 12 or 19. Consent for all the photographs was obtained from the families of the affected individuals.

very likely to be deleterious (as it results in a truncated protein), the c.2144C>T mutation is likely to be a rare polymorphism. Of note, subject 12, who presented an atypical facial appearance and indistinct hypoplastic nails, had two interstitial deletions at 6q25.3–q27 involving *ARID1B*, as detected by a SNP array (**Supplementary Fig. 6** and **Supplementary Methods**). Furthermore, subject 14 was found to have an interstitial deletion of *SMARCA2* by a SNP array (**Supplementary Fig. 7** and **Supplementary Methods**). No other copy-number changes involving genes encoding SWI/SNF complex components were found in subjects 2, 14 or 18 by array analysis. The overall mutation detection rate was 87%. In total, 20 of the 23 subjects had a mutation affecting one of the six SWI/SNF subunits.

Mutations in CSS were identified in the BAF-specific subunits *ARID1A* and *ARID1B* but not in PBAF-specific subunits (*BRD7*, *ARID2* and *PBRM1*) (**Supplementary Table 3**). In addition, mutations were identified in *SMARCA4* (*BRG1*) as well as in *SMARCA2* (*BRM*) (**Supplementary Table 3**). The BRG1 and BRM proteins are mutually exclusive catalytic ATP subunits in mammalian SWI/SNF complexes. Of note, the majority of heterozygous *Smarca4*-null mice survive with susceptibility to neoplasia, with a minority dying after birth because of exencephaly, whereas homozygous *Smarca2*-null mice are viable and fertile[4]. In *Smarca2*-null mice, Brg1 is upregulated, suggesting that Brg1 can functionally replace Brm in mice[10]. However, in humans, abnormalities in both *SMARCA4* and *SMARCA2* are found in CSS, indicating that the in-frame partial deletion of the gene encoding BRM in subject 19 has a specific mutational effect different from that of simple inactivation in mice. These data support the idea that abnormalities in the BRG1-BAF and BRM-BAF complexes can cause the abnormal neurological development in CSS.

All the mutated genes found in CSS, except for *SMARCE1*, have been reported to be associated with tumorigenesis[1,2]. Among the 23 subjects with CSS, only subject 3 with an *ARID1A* mutation presented with hepatoblastoma. To our knowledge, haploinsufficiency and/or homozygous inactivation of *ARID1A* have been found in several types of cancer but not in hepatoblastoma. Malignancies were not detected in any of the other subjects with CSS examined here. It remains to be seen whether malignancies are robustly associated with CSS.

Given the fact that all the mutations in *ARID1A* and *ARID1B* in CSS were predicted to cause protein truncation, we proposed that haploinsufficiency of these two genes must be able to cause CSS. cDNA analysis of lymphoblastoid cell lines from subjects 1, 6 and 23 indicated that the mutated transcripts were subject to nonsense-mediated mRNA decay (**Supplementary Fig. 8**). In subject 10, the *ARID1B* mutation associated with the creation of a premature stop codon in the last exon did not result in nonsense-mediated mRNA decay as expected (**Supplementary Fig. 8**).

In regard to the other mutated genes, germline heterozygous truncation mutations in *SMARCB1* and *SMARCA4* have been reported

Table 1 Mutations in individuals with Coffin-Siris syndrome

Subject ID	Gene	Mutation	Alteration	Type	Control allele frequency[a]
4	*SMARCB1*	c.1091_1093del AGA	p.Lys364del	*De novo*	0/502
11	*SMARCB1*	c.1130G>A	p.Arg377His	*De novo*	0/500
21	*SMARCB1*	c.1091_1093del AGA	p.Lys364del	NC	0/502
22	*SMARCB1*	c.1091_1093del AGA	p.Lys364del	NC	0/502
9	*SMARCA4*	c.1636_1638del AAG	p.Lys546del	*De novo*	0/350
7	*SMARCA4*	c.2576C>T	p.Thr859Met	*De novo*	0/368
5	*SMARCA4*	c.2653C>T	p.Arg885Cys	*De novo*	0/368
16	*SMARCA4*	c.2761C>T	p.Leu921Phe	*De novo*	0/368
25	*SMARCA4*	c.3032T>C	p.Met1011Thr	NC	0/372
17	*SMARCA4*	c.3469C>G	p.Arg1157Gly	*De novo*	0/368
19	*SMARCA2*	Partial deletion		*De novo*	–
24	*SMARCE1*	c.218A>G	p.Tyr73Cys	*De novo*	0/368
3	*ARID1A*	c.31_56del	p.Ser11Alafs*91	NC	0/330
6	*ARID1A*	c.2758C>T	p.Gln920*	NC	0/376
8	*ARID1A*	c.4003C>T	p.Arg1335*	*De novo*	–
1	*ARID1B*	c.1678_1688del	p.Ile560Glyfs*89	*De novo*	–
15	*ARID1B*	c.1903C>T	p.Gln635*	*De novo*	–
23	*ARID1B*	c.3304C>T	p.Arg1102*	*De novo*	–
10	*ARID1B*	c.2144C>T	p.Pro715Leu	NC	0/368
10	*ARID1B*	c.5632del G	p.Asp1878Metfs*96	NC	0/374
12	*ARID1B*	Microdeletion		NC	–

NC, not confirmed because parental samples were unavailable.
[a]The numbers indicate the observed allele frequency (alleles harboring the change/total tested alleles) in Japanese controls. None of the mutations was found in dbSNP132, the 1000 Genomes database or the National Heart, Lung, and Blood Institute (NHLBI) GO exomesequencing project database. –, not tested.

in individuals with rhabdoid tumor predisposition syndromes 1 (RTPS1; MIM 609322) and 2 (RTPS2; MIM 613325)[11,12], and various types of *SMARCB1* mutations (missense, in-frame deletion, nonsense and splice site) have been found in the germline of individuals with familial and sporadic schwannomatosis (MIM 162091)[13,14]. Furthermore, mice with heterozygous knockout of *Smarca4* or *Smarcb1* were prone to tumor development[2]. All the mutations in *SMARCA4* and *SMARCB1* in individuals with CSS were nontruncating (either missense or in-frame deletions), implying that they exert gain-of-function or dominant-negative effects (excluding haploinsufficiency as a cause). It is noteworthy that comparable germline mutations in *SMARCB1* have such different phenotypic consequences in their association with the phenotypes of CSS and schwannomatosis. The *SMARCB1* mutations in CSS and those in schwannomatosis are indeed different according to the Human Gene Mutation Database. With regard to the *SMARCA2* interstitial deletion in CSS, the change maintained the coding sequence reading frame but removed exons 20–27 that encode the HELICc domain. RT-PCR analysis confirmed the deletion of exons 20–27 at the cDNA level (**Supplementary Fig. 7**). These data suggest the importance of the HELICc domain in the SMARCA2 protein.

The various types of mutations in the genes encoding different SWI/SNF components resulted in similar CSS phenotypes. This suggests that the SWI/SNF complexes coordinately regulate chromatin structure and gene expression. This is the first report, to our knowledge, of germline mutations in SWI/SNF complex genes associated with a multiple congenital anomaly syndrome, highlighting new biological aspects of SWI/SNF complexes in humans. Similarly, genes encoding SNF2-related proteins, which are implicated as chromatin remodeling factors outside of SWI/SNF complexes, are mutated in different syndromes, including in α-thalassaemia/mental retardation syndrome X-linked (ATRX; *ATRX* mutations) and in coloboma, heart defect, atresia choanae, retarded growth and development, genital abnormality and ear abnormality (CHARGE) syndrome (*CHD7* haploinsufficiency)[3]. We expect that more mutations affecting chromatin remodeling factors will be found in different human diseases.

URLs. Human Gene Mutation Database, https://portal.biobase-international.com/cgi-bin/portal/login.cgi.

Note: Supplementary information is available on the Nature Genetics website.

ACKNOWLEDGMENTS

We thank all the family members for participating in this study. This work was supported by research grants from the Ministry of Health, Labour and Welfare (to N. Miyake, H.S. and N. Matsumoto), the Japan Science and Technology Agency (to N. Matsumoto), the Strategic Research Program for Brain Sciences (to N. Matsumoto), the Japan Epilepsy Research Foundation (to H.S.) and the Takeda Science Foundation (to N. Matsumoto and N. Miyake). This study was also funded by a Grant-in-Aid for Scientific Research on Innovative Areas (Foundation of Synapse and Neurocircuit Pathology) from the Ministry of Education, Culture, Sports, Science and Technology of Japan (to N. Matsumoto), a Grant-in-Aid for Scientific Research from the Japan Society for the Promotion of Science (to N. Matsumoto), a Grant-in-Aid for Young Scientists from the Japan Society for the Promotion of Science (to N. Miyake and H.S.) and a Grant for 2011 Strategic Research Promotion of Yokohama City University (to N. Matsumoto). This study was performed at the Advanced Medical Research Center at Yokohama City University. Informed consent was obtained from all the families of affected individuals. The Institutional Review Board of Yokohama City University approved this study.

AUTHOR CONTRIBUTIONS

Y.T., S. Miyatake, I.O., H.D., H.S. and N. Miyake performed exome sequencing and Sanger sequencing. Y.T., M.S., K.O., I.O., T.M., H.D., H.S. and N. Miyake performed data management and analysis. N.O., H.O., T. Kosho, Y.I., Y.H.-K., T. Kaname, K.N., H.K., K.W., Y.F., T.H., M.K., Y.H., T.Y., S.Y., S. Mizuno, S.S., T.I., T.N., T.O. and N.N. provided clinical materials after careful evaluation. Y.T., N. Miyake and N. Matsumoto wrote the manuscript. N. Matsumoto designed and oversaw all aspects of the study.

COMPETING FINANCIAL INTERESTS

The authors declare no competing financial interests.

Published online at http://www.nature.com/naturegenetics/.
Reprints and permissions information is available online at http://www.nature.com/reprints/index.html.

1. Reisman, D., Glaros, S. & Thompson, E.A. *Oncogene* **28**, 1653–1668 (2009).
2. Wilson, B.G. & Roberts, C.W. *Nat. Rev. Cancer* **11**, 481–492 (2011).
3. Clapier, C.R. & Cairns, B.R. *Annu. Rev. Biochem.* **78**, 273–304 (2009).
4. Bultman, S. *et al. Mol. Cell* **6**, 1287–1295 (2000).
5. Hargreaves, D.C. & Crabtree, G.R. *Cell Res.* **21**, 396–420 (2011).
6. Xue, Y. *et al. Proc. Natl. Acad. Sci. USA* **97**, 13015–13020 (2000).
7. Coffin, G.S. & Siris, E. *Am. J. Dis. Child.* **119**, 433–439 (1970).
8. Bamshad, M.J. *et al. Nat. Rev. Genet.* **12**, 745–755 (2011).
9. Wittwer, C.T., Reed, G.H., Gundry, C.N., Vandersteen, J.G. & Pryor, R.J. *Clin. Chem.* **49**, 853–860 (2003).
10. Reyes, J.C. *et al. EMBO J.* **17**, 6979–6991 (1998).
11. Schneppenheim, R. *et al. Am. J. Hum. Genet.* **86**, 279–284 (2010).
12. Taylor, M.D. *et al. Am. J. Hum. Genet.* **66**, 1403–1406 (2000).
13. Boyd, C. *et al. Clin. Genet.* **74**, 358–366 (2008).
14. Hadfield, K.D. *et al. J. Med. Genet.* **45**, 332–339 (2008).